Advances in Concrete Construction, *Vol. 10, No. 1 (2020) 21-34*
DOI: https://doi.org/10.12989/acc.2020.10.1.021

Crack width control of precast deck loop joints for continuous steel-concrete composite girder bridges

Changsu Shim[a] and Chidong Lee*

Department of Civil Engineering, College of Engineering, Chung-Ang University, 84 Heukseok-ro, Dongjak-gu, Seoul 156-756, Republic of Korea

(*Received February 8, 2019, Revised June 14, 2020, Accepted June 15, 2020*)

Abstract. Precast deck joints have larger crack width than cast-in-place concrete decks. The initial crack typically occurs at the maximum moment but cracks on precast joints are significant and lead to failure of the deck. The present crack equation is applied to cast-in-place decks, and requires correction to calculate the crack width of precast deck joints. This research aims to study the crack width correction equation of precast decks by performing static tests using high strength and normal strength concrete. Based on experimental results, the bending strength of the structural connections of the current precast deck is satisfied. However it is not suitable to calculate and control the crack width of precast loop connections using the current design equation. A crack width calculation equation is proposed for crack control of precast deck loop joints. Also included in this paper are recommendations to improve the crack control of loop connections.

Keywords: loop joint; crack width; precast deck; high strength concrete; static test

1. Introduction

Currently, there are many public bridges that are over 40 to 50 years old. Many are nearing the end of their designed life cycle while some have already surpassed it. The portion of the bridge most likely to age quickly is the deck, because vehicle load and weather changes directly affect the deck, while the girder is relatively less affected (Lewis 2009, Shim *et al*. 2010). Therefore, girder maintenance and repair methods for changing the entire deck have been studied. At the time of their construction, many bridges were built in rural areas, but owing to accelerated urbanization, it is now common that bridges are present in city areas. If the time to repair a bridge is delayed, then the urbanized location surrounding the bridge results in problems such as traffic congestion, dust, and noise. To minimize these issues, a precast technique is applied, in which components are fabricated in factories located away from the site, and components can be easily installed on site. This in turn can save time and construction costs, reduces traffic disturbance, improves workability and ensures quality control (Hallmark *et al*. 2012). Despite these beneficial effects, many researches have reported problems with usability and durability of precast components, such as cracking of precast connections and corrosion of steel by water (Issa *et al*. 1995).

Extensive researches and case studies on various types of precast joints such as post-tensioning, loop joint, lap splice and headed reinforcement have already been performed (Issa *et al*. 1995, Shim *et al*. 2000, Ryu *et al*. 2007, Joergensen and Hoang 2013, Kim *et al*. 2013, Joergensen and Hoang 2015, Shin *et al*. 2015, Kim and Shin 2016). The ultimate behaviour of a looped precast deck is similar to that of a reinforced concrete (RC) deck without joints. However as shown in Fig. 1, after a crack has occurred owing to an applied load, the precast deck joint with loop, PD300N-AVG, will have a larger crack width than the RC deck slab without a joint, ID-N-AVG, before reaching its ultimate strength.

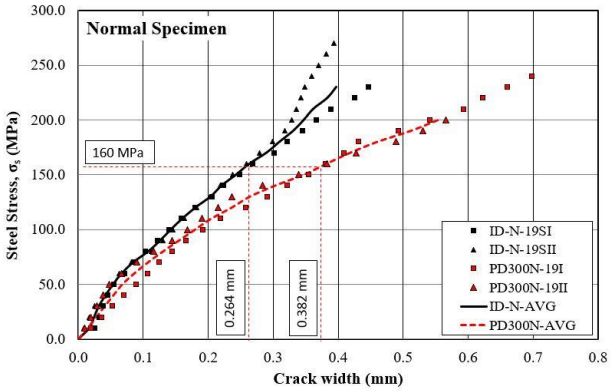

Fig. 1 Comparisons of steel stress - crack widths of precast and cast in situ

The precast deck system is used in many countries for accelerated deck slab replacement construction because it ensures high quality and minimizes formworks (Shim *et al*. 2010, Ma *et al*. 2015, Gillen *et al*. 2018). However, increased crack widths can lead to reduced durability. To solve this problem, post-tensioning systems can be introduced across precast joints, but it is difficult to design

*Corresponding author, Ph.D.
E-mail: doinda@hanmail.net
[a]Professor
E-mail: csshim@cau.ac.kr

ISSN: 2287-5301 (Print), 2287-531X (Online)

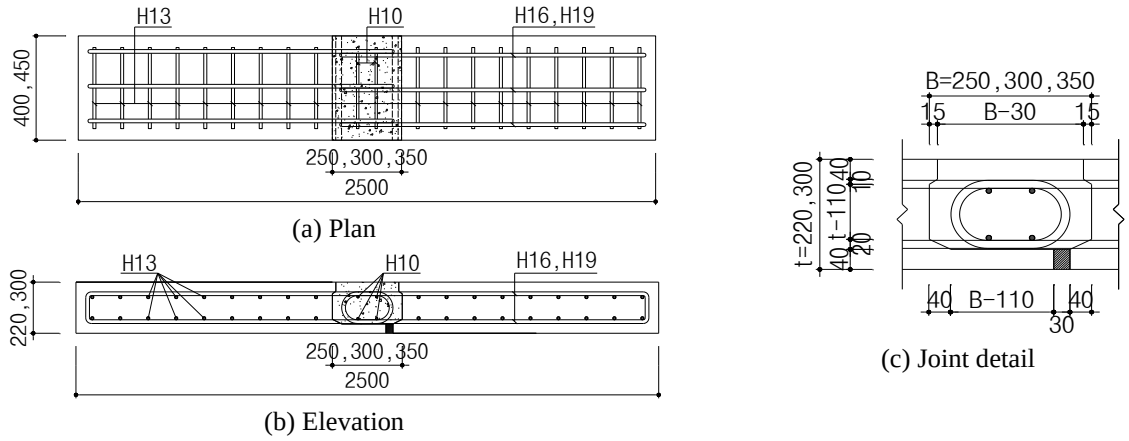

Fig. 2 Schematic diagrams of designed specimens.

Table 1 Main variables of test specimens

Specimen	Diameter of Loop (mm) / Yield Stress (MPa)	Joint Spacing *B* (mm)	Slab Width *W* (mm)	Slab Thickness *t* (mm)	Concrete Cover *c* (mm)	Joint Fill Compressive Strength (MPa)
PD250-16S	16 / 400	250	450	220	42	130
PD250-19S	19 / 400	250	450	220	40.5	130
PD300-16S	16 / 400	300	450	220	42	130
PD300-19S	19 / 400	300	450	220	40.5	130
PD350-16S	16 / 400	350	450	220	42	130
PD350-19S	19 / 400	350	450	220	40.5	130
PD300-22S	22 / 400	300	400	300	29	40
PD300-22C	22/ 400	300	400	300	29	40
PD300-22B	22 / 400	300	400	300	29	40

S: steel brushing, C: chipping, B: bond adhesive coating

and later replace this type of system in precast decks. Also, the induced stress by pre-stressing in the axial direction is reduced by creep and shrinkage.

Many research studies on factors influencing crack width have already been performed, such as reinforcement ratio and diameter, joint spacing, and strength of concrete. In calculating the crack widths, the effects of reinforcement are more significant than the effects of concrete strength (Creazza and Russo 1999). For precast decks with loop connections, the crack width is mainly affected by the diameter of the rebar (Ryu *et al*. 2007).

In this study, an evaluation was performed to define the crack behaviour at the joints of precast members and to establish the validity of design codes for calculating the crack width. To account for the increased in crack width, the modified crack width equation was developed. High strength concrete and normal strength concrete were each used as filler concrete for joints, and various conditions such as rebar diameter and joint spacing were chosen to investigate appropriate approaches to control cracks.

2. Experimental program

The main purpose of this experimental program was to evaluate the bending behavior of a looped precast deck slab filled with high strength concrete. Cracks and crack widths based on the stress level of tensile reinforcement to evaluate crack widths of precast loop joints were also of major interest in the experiments (Ji 2014).

2.1 Details of test specimens

The loop connection details are designed using a precast deck slab of full depth to allow construction without any formwork, as shown in Fig. 2(c). The reason why the lower protrusion element of the pocket was biased is that the precast slab cannot be installed because of interference with the reinforcement if it is placed symmetrically in the middle. The specimen is 2.5 m long and has nine different joint details, as shown in Table 1. PD250-16 to PD350-19 specimens were made (450 mm wide and 220 mm depth). In addition, PD300-22S to PD300-22B specimens were made (400 mm wide and 300 mm depth). Longitudinal loop reinforcements used were 16 mm, 19 mm, and 22 mm, with 10 mm lateral reinforcement across the loop core. Waterproof rubber was installed to prevent leakage of cement paste between the two precast elements, as shown in Fig. 2(c).

The anchoring criteria for compression and tension of the reinforcement were compared for Eurocode 2 (EN1992-1-1), ACI 318 (2014), and DIN 1045. As ACI 318 is an anchor equation, it is considered to be a lap splice by multiplying its value by 1.3. From the review as shown in Table 2, most design basis-based joints using these codes are calculated to be larger than the joints we used. Our

Table 2 Comparison of lap splice length to code

Specimen	Diameter of Loop (mm)	Designed Concrete Compressive Strength for Joint (MPa)	Calculated development length (mm)			Lap Splice Length of each Specimen (mm)
			EC2	DIN 1045	ACI 318-14	
PD250-16S	16	130	240	235	176	220
PD250-19S	19	130	285	279	208	220
PD300-16S	16	130	240	235	176	220
PD300-19S	19	130	285	279	208	220
PD350-16S	16	130	240	235	176	220
PD350-19S	19	130	285	279	208	220
PD300-22S	22	40	657	404	460	272
PD300-22C	22	40	657	404	460	272
PD300-22B	22	40	657	404	460	272

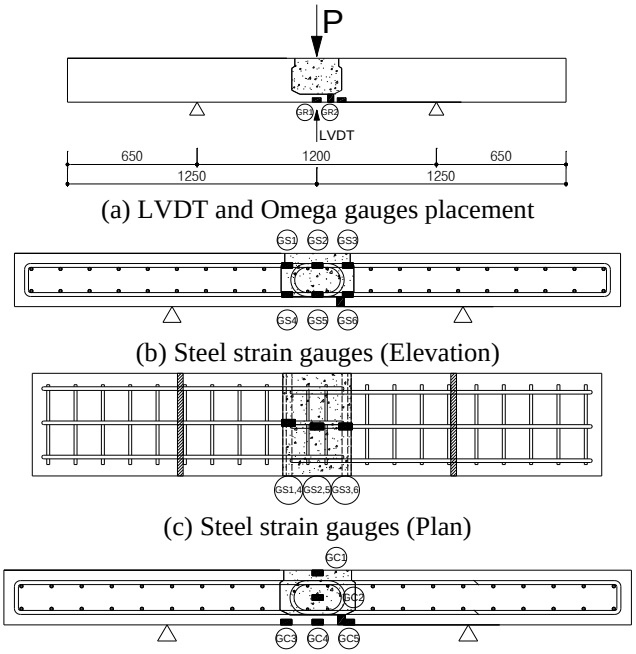

(a) LVDT and Omega gauges placement

(b) Steel strain gauges (Elevation)

(c) Steel strain gauges (Plan)

(d) Concrete strain gauges (Elevation)

Fig. 3 Measurement plan

connections were tested at 250 mm, 300 mm, 350 mm widths, which are smaller than the widths obtained by calculation, because larger joints would reduce constructability, increase the construction period, and reduce the unique advantages of a precast deck slab that is superior in quality control.

2.2 Material properties

The experimental program used two types of concrete to fill the connections. One is normal strength concrete with design strength of 40 MPa and the other is high strength concrete with design strength of 130 MPa.

The properties of high-strength concrete on the joints were determined by ASTM test methods. The compressive strength test was performed with ASTM C109 (modified); the elastic modulus with ASTM C469; and the flexural strength with ASTM C1609. The corresponding mechanical property values are 130 MPa, 43,000 MPa and 9.4 MPa, respectively. Values were taken as the average of three samples of each test. The compressive strength and elastic modulus tests were performed on the 28th day of curing.

The recorded compressive strengths of concrete on the precast member are 53 MPa for high-strength concrete at joint fill and 51 MPa for normal-strength concrete at joint fill on the 28th day of curing. The concrete compressive strengths of the joint fill are 136 MPa for high-strength and 51MPa for normal-strength. Reinforcement with diameters 16 mm, 19 mm, and 22 mm, has yield strength of 400 MPa.

2.3 Measurement plan and loading

Three-point load static tests were performed to investigate bending strength and crack behavior. For this purpose, a crack width measurement of each test was performed using a line variable variation transducer (LVDT), six steel strain gauges, five concrete strain gauges, and two omega gauges. Fig. 3 shows the measurement plan adopted for the experimental program. The LVDT was placed below the middle of the span, where the maximum deflection occurred. To measure the crack width, two omega gauges were attached to the concrete surface where the initial crack appeared during the test.

All specimens were simply supported, as shown in Fig. 4. The support points were symmetrically located 650 mm away from each end of the precast member. As illustrated in Fig. 4, a hydraulic device with a capacity of 2000 kN was used to produce a single vertical load at the middle point of each specimen.

The load on all specimens was controlled according to the following procedure. After stabilization of the applied load by means of repeated loading and removing, a specimen was reloaded using a load control method (0.5 kN/s) until the initial crack was observed. Then, the load applied to a specimen was removed to install the two omega gauges on the surface where bending cracks were observed. After attaching the omega gauges, loading continued and the load control method was changed to a displacement control method (1 mm/min) until the specimen was fractured. During the test, crack progress was recorded on the surface of each specimen, and data regarding displacement and strain of the concrete and the reinforcement were recorded using data loggers. In addition, the failure mode of the specimen was sufficiently observed.

3. Test results and discussion

The experimental program was performed to evaluate the structural behavior of the loop joints, including the

Fig. 4 Test setup

Table 3 Ultimate flexure strengths and failure modes

Specimen	Ultimate Strength			Calculated Shear Strength (kN)	Failure Mode
	Experiment (kN)	Calculated Nominal Flexural Strength (kN)*	Experiment / Calculation		
PD250-16S	228	132 (M) / 166 (I)	1.73 (M) / 1.37 (I)	148	Flexural
PD250-19S	227	188 (M) / 237 (I)	1.21 (M) / 0.96 (I)	148	Flexure + Shear cracks
PD300-16S	245	132 (M) / 175 (I)	1.86 (M) / 1.40 (I)	148	Flexural
PD300-19S	346	188 (M) / 250 (I)	1.84 (M) / 1.38 (I)	148	Flexural
PD350-16S	218	132 (M) / 186 (I)	1.65 (M) / 1.17 (I)	148	Flexural
PD350-19S	339	188 (M) / 265 (I)	1.80 (M) / 1.28 (I)	148	Flexural
Average			1.78 / 1.32	PD250-19 was excluded	
PD300-22S	361	254 (M) / 340 (I)	1.42 (M) / 1.06 (I)	198	Flexural
PD300-22C	390	254 (M) / 340 (I)	1.54 (M) / 1.15 (I)	198	Flexural
PD300-22B	343	254 (M) / 340 (I)	1.35 (M) / 1.01 (I)	198	Flexural
Average			1.44 / 1.07		

*(M): Mid-section, (I): Interface-section

ultimate load capacity, failure modes, and the formation and propagation of cracks.

3.1 Flexural strength

A specimen was designed so that the concrete during compression reaches failure after the reinforcement reaches its yield strength, resulting in ductile failure. Before the static experiment, the flexural strength was calculated in advance using the criterion in Eurocode-2, and then the calculated ultimate strength was compared with the test results. Table 3 shows a comparison of the ultimate strength corresponding to the ultimate flexural strength tested and the ultimate bending strength by calculation. For the mid-span section, the ultimate strength of a specimen filled with high-strength concrete was 78% higher than the calculated value, while a specimen filled with normal strength concrete showed a 44% higher strength. At the precast interface, the flexural strength was relatively low, so for the central part, the ultimate strength of the specimen filled with high strength concrete was 32% higher than the calculated value, and the specimen filled with normal strength concrete was 7% higher. All of the experiments indicated sufficient ultimate strength, therefore it can be said that the details of the loop joints used in the experimental program had adequate anchorage length for the required strength.

Table 4 Cracking strengths

Specimen	Cracking Strength		
	Experiment (kN)	Calculation (kN)	Experiment/ Calculation
DD250-16	82	47	1.74
DD250-19	78	47	1.66
DD300-16	95	50	1.9
DD300-19	80	50	1.6
DD350-16	105	53	1.98
DD350-19	105	53	1.98
DD300-22S	35	101	0.44
DD300-22C	Occurred before test	101	-
DD300-22B	Occurred before test	101	-

3.2 Crack and failure modes

The initial crack load depends on the width of the joint, as the calculation of the initial crack strength is based on the location of the initial crack at the interface of the boundary. Thus, the crack moment of each specimen is proportional to the distance from the midpoint to the interface between the precast slab and the filler.

Table 4 shows the comparison of cracking load between measured values and calculated values. In the experiment, the strength of the crack was determined based on the load values acting upon the initial crack. For all experiments, initial cracks were observed near the interface, and cracks were generated under applied load values between 75 kN and 105 kN. The crack strength is approximately 1.45 times greater than the calculated value. In experiments with normal strength concrete deck, an initial crack occurred during the transportation and installation process.

However, specimens filled with high-strength concrete have significantly improved crack strength/resistance, as summarized in Table 4. Specimens with wide joint distances showed a slight increase in crack strength. Thus, for better quality control of loop joints, it is recommended to use high strength filler concrete and wide loop joints. It is difficult to prevent cracks in specimens filled with normal strength concrete in the loop joints after the concrete has been cast.

Fig. 5 shows the forms of cracks in each specimen and the final failure mode. During the experiments, it was observed that initial cracks always occurred at the interface of the boundary, although the maximum moment occurred at the middle of the span. For each specimen, after the

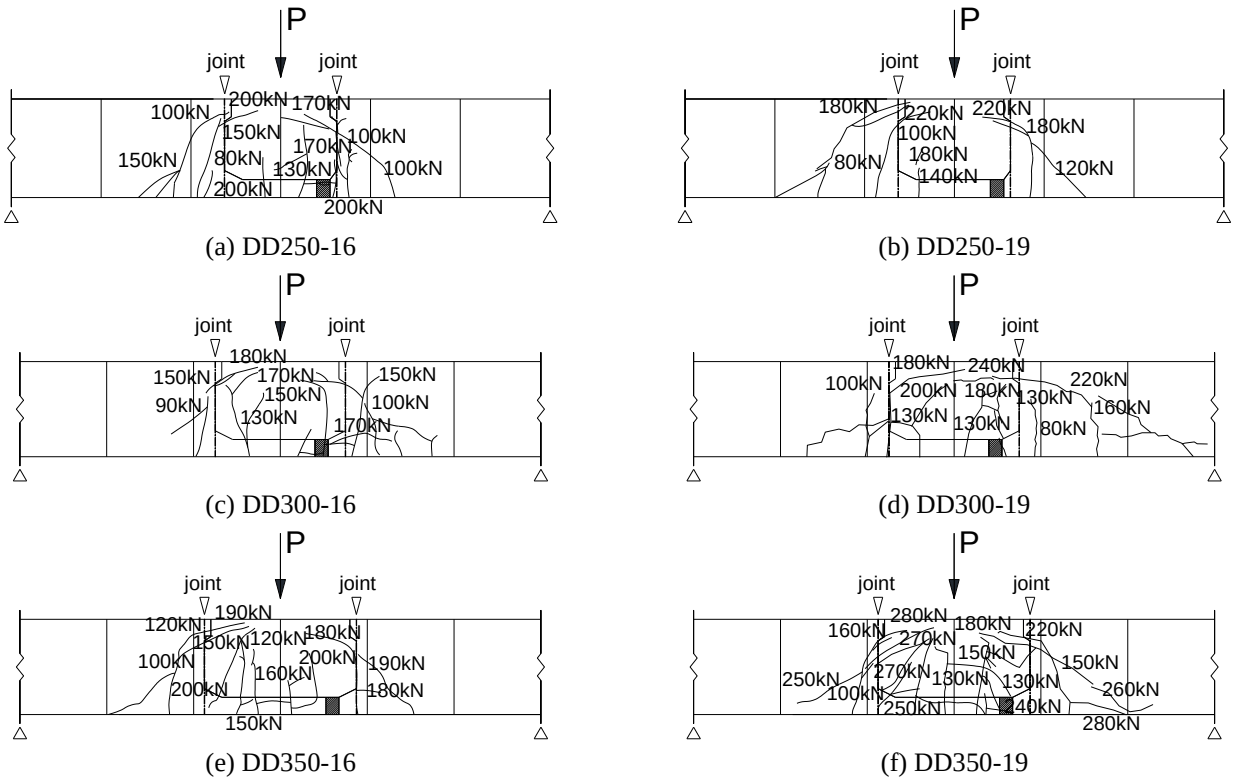

(a) DD250-16 (b) DD250-19

(c) DD300-16 (d) DD300-19

(e) DD350-16 (f) DD350-19

Fig. 5 Cracking patterns and failure modes

initial crack, the vertical crack propagates toward each end. When the applied load approached the ultimate load, a distribution of diagonal cracks in the compression area was observed. As the load increased, the crack width also increased, ultimately leading to the specimen's failure. All of the specimens showed a pattern of cracks distributed in both the joint and precast slab in the failure mode. Therefore, this phenomenon proves that the reinforcement is well anchored in the concrete and that the anchorage length of the reinforcement is sufficient to produce the desired strength.

In addition to observation of the initial cracks and identification of the location of a crack from the load-deflection curve, the initial crack point was identified with a steel strain graph for each specimen, as shown in Fig. 6. In each graph, the slope of the specimen with high strength concrete was linear before the crack. However, the slope became flat after the yielding point. For a specimen with normal strength filler concrete, the tensile stress of the reinforcement gradually increased, as shown in Fig. 6(b). In addition, the steel strain was very high. This means that the load borne by the reinforcements increases rapidly after failure of the concrete accompanying the initial crack generation. However, after the initial crack, the steel strain of the specimen with a joint width of 350 mm did not increase relative to that of the other experiments. The stress of a specimen with a 350 mm joint was only 60 MPa, while the other specimens showed a stress of approximately 200 MPa. Flexural cracks occurred almost simultaneously with the initial crack in the joints and in the middle of the 350 mm joint specimen. Therefore, to avoid stress concentration at the joints, it is recommended to use a 350 mm joint

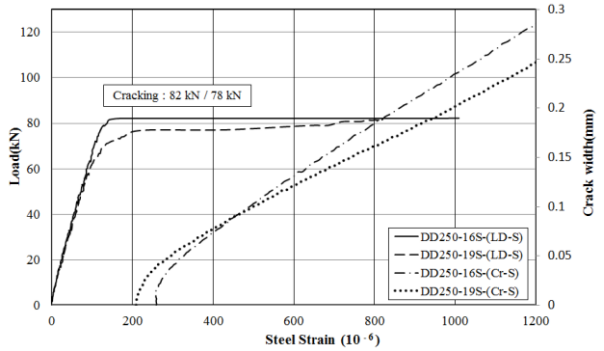

(a) DD250 series

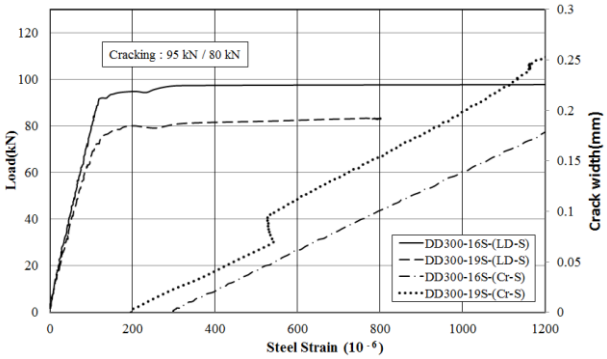

(b) DD300 series

Fig. 6 Steel-strain curves according to diameter of loop reinforcements

width. This width also induces the distribution of bending cracks in the event of a crack because high strength concrete was used as the filler for the loop joint.

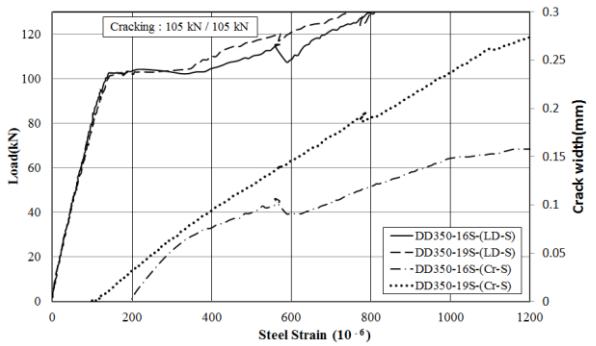

(c) DD350 series

LD-S: Load – Steel Strain curve, Cr-S: Crack width – Steel Strain curve

Fig. 6 Continued

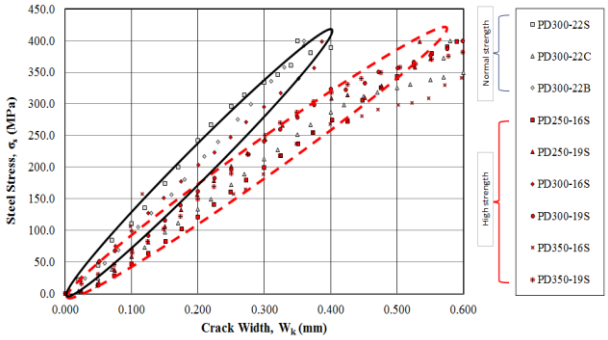

Fig. 7 Comparison of reinforced stress-crack width by specimen.

4. Crack width control of precast deck joints

4.1 Crack width effect by precast loop joint shape

Joints of precast members are weak at the interface between precast concrete and filler concrete, and cracks are inevitable. If the experiment results are plotted with respect to reinforcement stress-cracking width, Fig. 7 is the result and the curves can be divided into two types. The first type is the result of an experiment using specimens filled with high-strength concrete (enclosed with an elliptical dashed-line), where the high tensile strength of the high-strength concrete (130 MPa) causes a narrow crack width for the same level of steel stress in each specimen. The second type is the experiment enclosed with an elliptical line for normal strength concrete filler. In particular, the width of cracks is narrower than for specimens filled with high-strength concrete for the same level of reinforcement stress, despite the lower strength of the filler concrete. In Fig. 7, the crack width between the two groups of specimens is closely related to the bend geometry of the loop reinforcement. As shown in Fig. 8, specimens filled with high-strength concrete have a high curvature of the loop (semi-circular in shape), while those filled with normal-strength concrete have a low curvature owing to the rapid bend of the loop shape. The specimen of Fig. 8(a) has a diameter of 16 mm and 19 mm, and the specimen of Fig. 8(b) has a diameter of 22 mm. Although the ratio of used to required loop length of Fig. 8(b) is shorter than Fig. 8(a), the crack width in Fig. 8(a) is narrower than in Fig. 8(b). The reason is because of the long direct lap joint length of the loop reinforcements, as shown in Fig. 9.

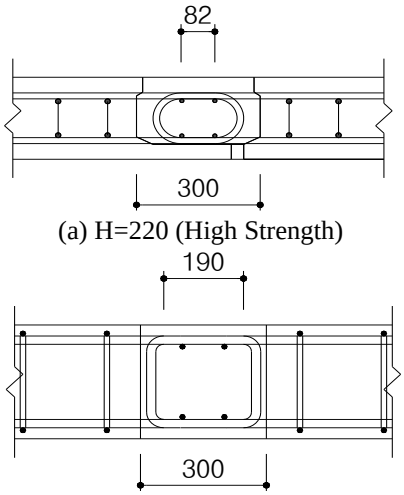

(a) H=220 (High Strength)

(b) H=300 (Normal Strenght)

Fig. 8 Comparison of loop joint reinforcement.

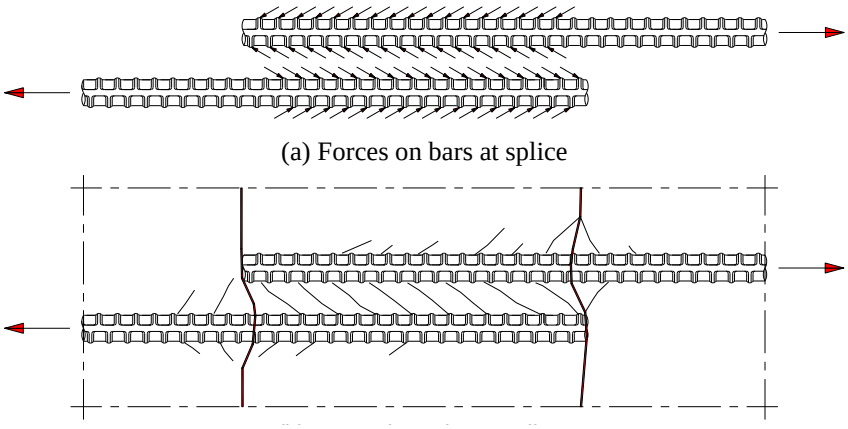

(a) Forces on bars at splice

(b) Internal cracks at splice

Fig. 9 Non-contact lap splice force transfer mechanism.

4.2 Modified crack width equation for the precast loop joint

Precast loop joints require their own crack width calculation equation, because the crack width at the interface of the precast to the filler was observed to be greater than that of the general slab and no design code is available. The proposed crack width calculation equation is derived based on the equation of Eurocode-2 by considering the following correction factors.

- Modification of maximum crack spacing considering the crack concentration at the interface of the joints
- Modification of crack width considering lack of a loop joint
- Modification of the crack width considering the shape of the loop reinforcement
- Crack width control considering filler concrete strength

The study on crack width and spacing of non-joint member is well studied by several researchers such as Bazant (1983) and Beeby (1970), (1971), (1979). The calculation of the crack width in Eurocode-2 is defined by multiplying the maximum crack spacing and the difference of strain between reinforcements and concrete, as shown in Eq. (1).

$$w_k = s_{r,max}(\varepsilon_{sm} - \varepsilon_{cm}) \tag{1}$$

The proposed modified maximum crack spacing equation reflects the larger width of the crack at the interface as the load increases, even if the initial crack in the specimen occurs at the maximum negative moment point. As the maximum crack spacing becomes the distance between the interface and the interface of the precast slab and filler, the conditions to consider the joint spacing, l_{JT}, were added. The method considered was to apply a larger value by comparing the maximum crack spacing by calculation, $s_{r,\max}$ and joint spacing, l_{JT}, as shown in Fig. 10. Because the deck slab's spacing of bonded reinforcement in the tensile zone is always less than $5(c + \emptyset/2)$, the maximum crack spacing, $s_{r,\max}$, can be calculated by Eq. (2). Crack spacing is a function of concrete tensile strength, adhesion stress distribution, reinforcement diameter, the steel cross section, and the effective tensile concrete area.

$$s_{r,max} = k_3 c + k_1 k_2 k_4 \phi/\rho_{eff} \geq l_{JT} \tag{2}$$

where, c is the cover of the concrete and ϕ is the diameter of the reinforcement.

The crack width is modified by considering the lack of a loop joint lap length and the shape of the loop reinforcement. The precast construction method is applied to improve constructability. If the size of the joints increases, the original quick and easy construction concept is decreased. Therefore, the width of precast loop joints currently used are planned and studied on a smaller scale than the joint length presented in Eurocode-2. However, reducing the size of the joints causes problems with increasing crack width even though the joint section satisfies the strength of the joint, because the joint length is not satisfied by the provision in the code. Therefore, the crack width equation is modified by the relationship between the required joint width given by Eurocode-2 and the actual joint width used. The modification of the crack width considering the shape of the loop reinforcement of the direct lap length is considered to be the biggest factor in crack width. Therefore, the crack width is modified by reflecting the effects considered.

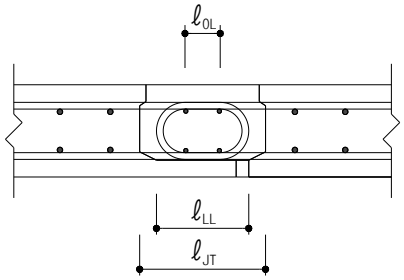

Fig. 10 Computational variables of loop joints

The ultimate bond stress for reinforcement, f_{bd}, as shown in Eq. (3) can be found as an expression of average tensile strength of concrete f_{ctm}. The coefficient η_1 (related to the location of the rebar in concrete) is 1.0 if the location of the reinforcement is good, and the coefficient η_2 relative to the diameter of reinforcement is 1.0 if the diameter of the reinforcement is less than 32.

$$f_{bd} = 2.25\eta_1\eta_2 f_{ctd} = 1.05 f_{ctm} \tag{3}$$

The design development length is calculated by Eq. (4). In this case, the effect of the form of the bars assuming adequate cover, α_1, is 1.0, for the effect of concrete minimum cover, α_2 is 1.0, for the effect of confinement by transverse reinforcement, α_3 is 1.0, for the effect of the pressure transverse to the plane of splitting along the design anchorage length, α_5 is 1.0, and for the lap length, α_6 is 1.5 for design purposes.

$$l_0 = \alpha_1\alpha_2\alpha_3\alpha_5\alpha_6 l_{b,rqd} = \frac{3\phi f_y}{14 f_{ctm}} \tag{4}$$

The crack width modified equation considering the lack of a loop joint and the shape of the loop reinforcement is as follows. l_{OL} is the direct overlap length of the the loop joint, l_{LL} is the used joint length of the loop reinforcement, as shown in Fig. 10. D is the outer bend diameter of the loop reinforcement $(2\mathrm{R} + \phi)$, and γ is an experimental variable. To compare the calculated crack width with the experimental value, we evaluate γ as 6/6, 7/6, and 8/6, as shown in Fig. 11. The calculated reinforcement stress to crack width slope is changed at 200 MPa in the precast member, so the experimental modified factor, γ is applied as 7/6 to control the crack width because the desired width is satisfied for 200 MPa or higher.

$$\begin{aligned} w_k &= s_{r,max}(\varepsilon_{sm} - \varepsilon_{cm})\frac{3}{14 l_{LL}}\frac{\phi f_y}{f_{ctm}}\left(1 - \frac{l_{OL}}{l_{LL}}\right) \\ &= s_{r,max}(\varepsilon_{sm} - \varepsilon_{cm})\gamma\left(\frac{3}{14}\frac{\phi f_y}{f_{ctm}}\right)\left(\frac{D}{l_{LL}^2}\right) \\ &= s_{r,max}(\varepsilon_{sm} - \varepsilon_{cm})\left(\frac{\phi f_y}{f_{ctm}}\right)\left(\frac{D}{4\, l_{LL}^2}\right) \end{aligned} \tag{5}$$

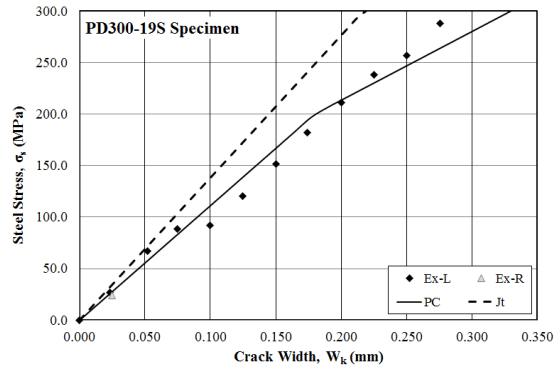

(a) γ =6/6

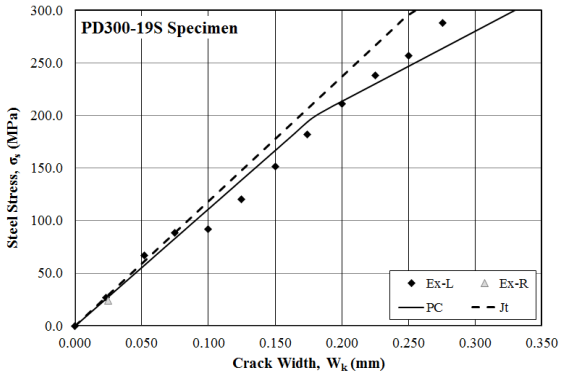

(b) γ =7/6

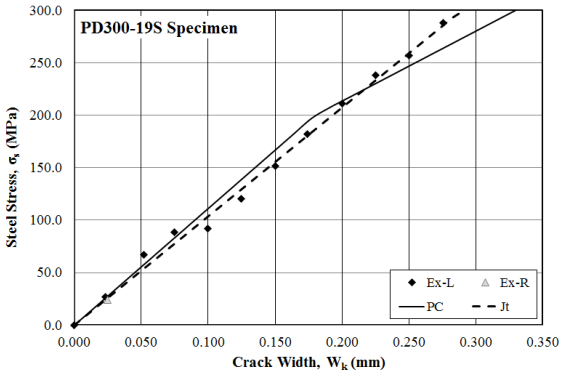

(c) γ =8/6

Fig. 11 Comparisons of steel stress to crack width for different variation factors

The difference in strain is calculated as shown in Eq. (6) and the calculated value is defined to be at least 60% of the steel yielding strain.

$$\varepsilon_{sm} - \varepsilon_{cm} = \frac{\sigma_s - k_t \frac{f_{ct,eff}}{\rho_{p,eff}}\left(1 + \alpha_e \rho_{p,eff}\right)}{E_s} \geq 0.6\frac{\sigma_s}{E_s} \quad (6)$$

5. Crack width control of loop joints in steel-concrete composite girder bridges

The modified crack width calculation derived in Chapter 4 is now applied to typical steel-concrete composite girder bridges. The load resistance factored design method

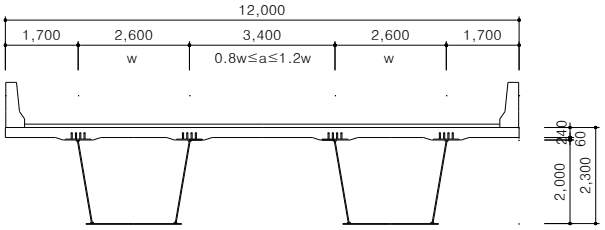

Fig. 12 Typical section of steel-concrete composite girder

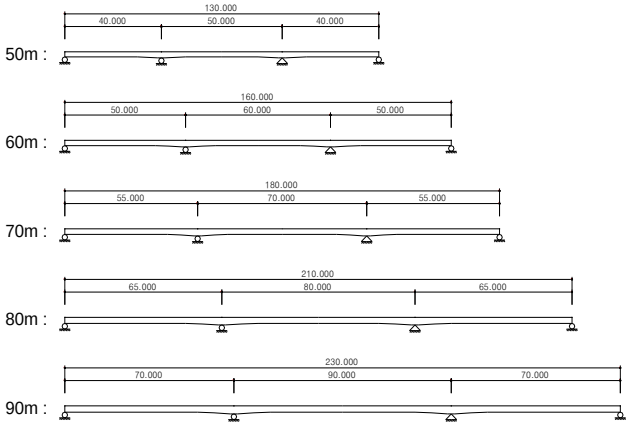

Fig. 13 Span configuration of the bridges

requires that the axial reinforcement of the deck slab shall cover at least 1% of the cross sectional area, and provisions concerning the actual calculation of the deck slab reinforcements are not given in the design basis. However, after composition, the deck slab of the steel-concrete composite girder is subjected to tensile stress on the deck slab caused by shrinkage and the secondary dead load. In addition, the tensile stresses applied on the deck slab by the increment of the span length increase. Nevertheless, cracks in precast joints may intensify, as the girder deck slab is designed with the precast loop connection. Although there is no problem immediately after construction, as time elapses after completion, cracks in precast joints may intensify. Cracks on precast joints can cause leakage and corrosion of the reinforcement owing to penetration of de-icing salts in winter, thereby reducing the durability of the girder deck slab. Nevertheless, reinstallation of girder deck slabs in urban areas requires the precast method to minimize the construction period and minimize the joint width. Therefore, the crack width of the precast deck slab can be controlled by using the modified crack width calculation method derived in Chapter 4 and by using high strength concrete filler.

5.1 Dimensions of the bridge

The designed bridge is a steel-concrete composite tub-girder bridge, as shown in Fig. 12, on which a parametric study was performed by increasing the span length from 50 m to 90 m in 10 m increments, as shown in Fig. 13 and Table 5. The method of this study determined the girder dimension in the same way as in actual design, and the deck slab was evaluated with the axial forces generated by creep, shrinkage, secondary dead load, and a live load of 30% on

Table 5 Girder depth to span length

Span Length (m)	Girder Depth (m)	
	Mid Span	Support
50	2.3	2.7
60	2.4	2.8
70	2.5	3.1
80	2.7	3.3
90	2.8	3.5

determined girder sections. The cross section of the steel-concrete composite girder had a web plate slope of 1:6. The center-to-center distance of inner webs of the adjacent boxes, "*a*" shall be 80~120% of the center-to-center distance of each box, "*w*", as stipulated by AASHTO LRFD. However this provision is not applied, therefore the analysis is performed by three-dimensional analysis.

Table 6 Moment diagram

Stage	Moment Diagram
Construction stage	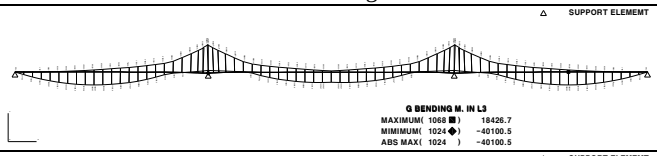
Service stage (Before composite)	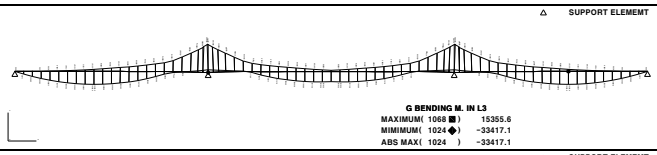
Service stage (After composite)	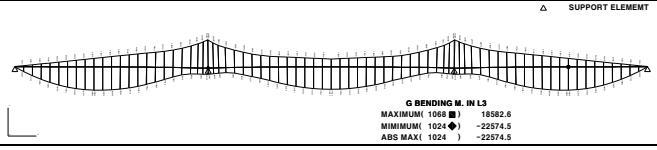

Table 7 Moment ratio for each limit state

Items	Section checked
Construction stage	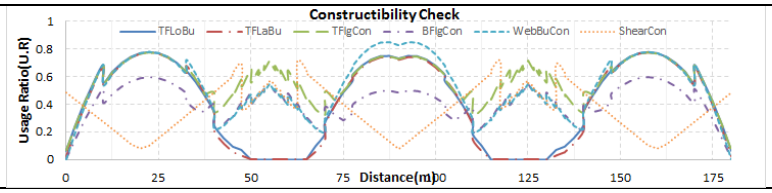
Results	· Maximum U.R of positive moment: U.R=77.7% .∴. O.K · Maximum U.R of negative moment: U.R=71.8% .∴. O.K
Service Limit State	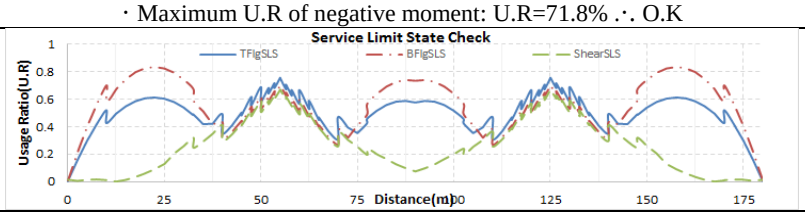
Results	· Maximum U.R of positive moment: U.R=83.4% .∴. O.K · Maximum U.R of negative moment: U.R=75.5% .∴. O.K
Fatigue Limits State	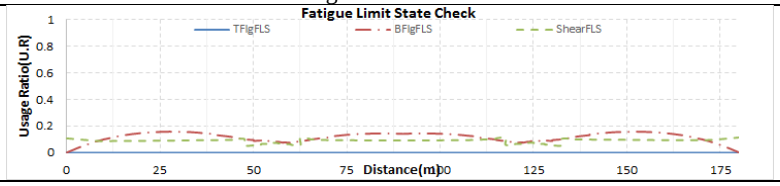
Results	· Maximum U.R of positive moment: U.R=16.0% .∴. O.K · Maximum U.R of negative moment: U.R=11.2% .∴. O.K
Strength Limits State	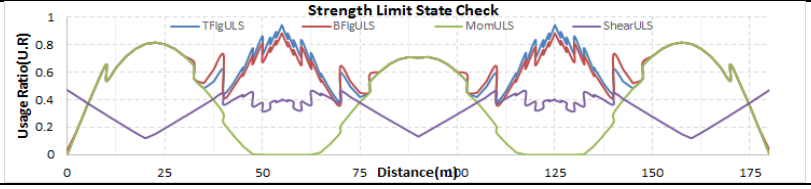
Results	· Maximum U.R of positive moment: U.R=81.5% .∴. O.K · Maximum U.R of negative moment: U.R=94.2% .∴. O.K

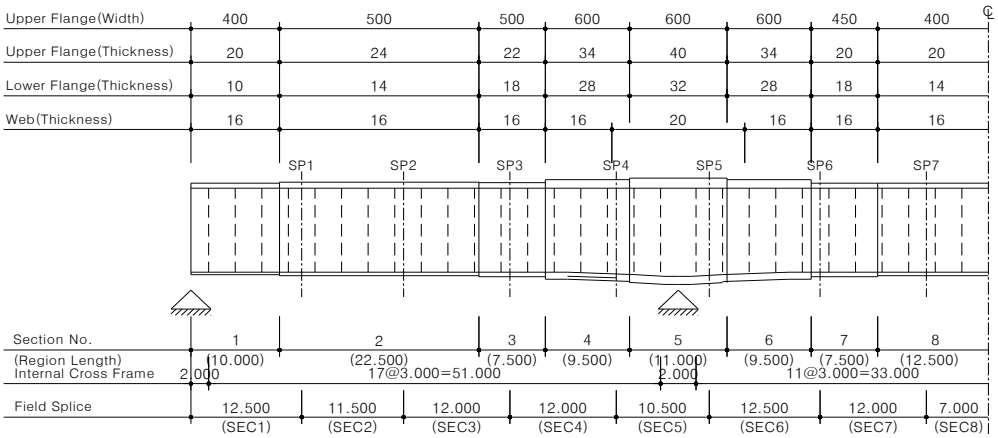

Fig. 14 Plate thickness of 70 m main span bridge

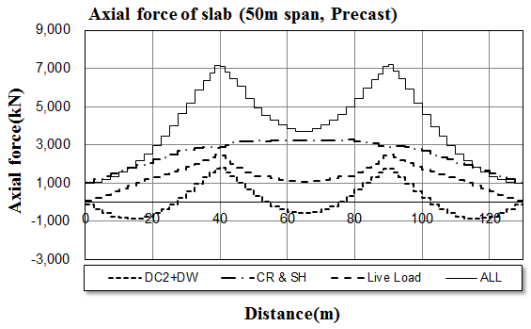

(a) 50 m span

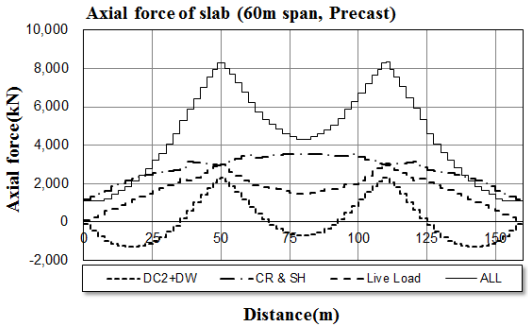

(b) 60 m span

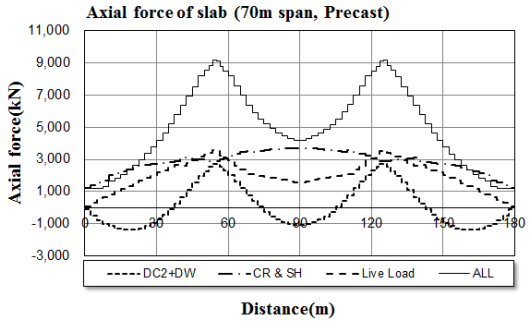

(c) 70 m span

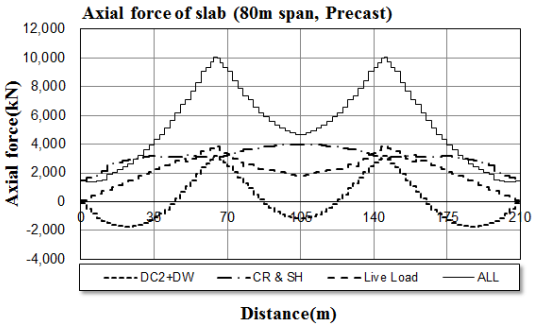

(d) 80 m span

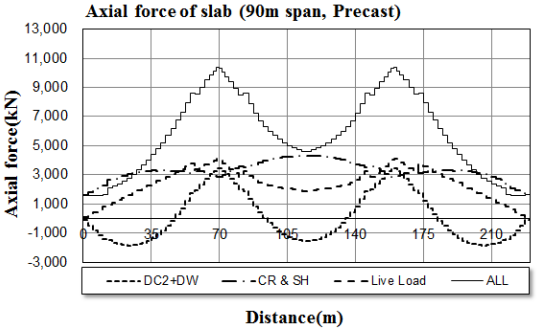

(e) 90 m span

Fig. 15 Axial force applied to slab in the longitudinal direction

5.2 Design results of the bridge (70 m class)

Structural calculations of steel-concrete composite tub-girders are checked for safety review, service limit states, fatigue limit states, and strength limit states. The member force for the cross-sectional check is divided into the construction stage and service stage, and the latter is divided into before and after composition. Table 6 presents a moment envelope diagram and Table 7 is the usage ratio for each limit state. Fig. 14 is a steel plate thickness

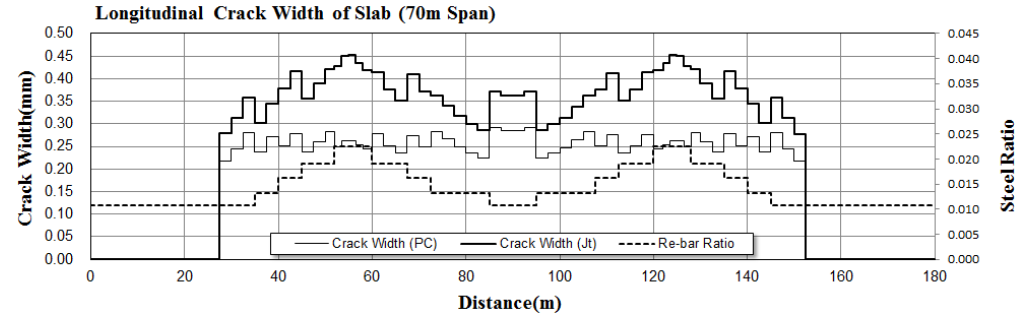

(a) Normal strength concrete filler case (70 m span)

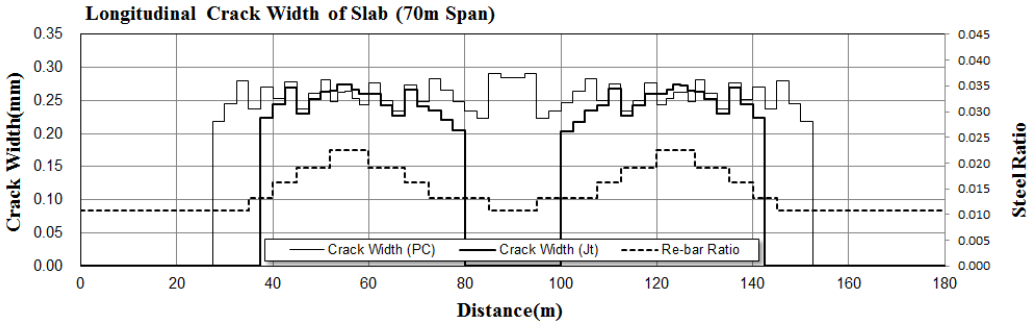

(b) High strength concrete filler case (70 m span)

Fig. 16 Comparisons of slab crack width (Normal vs. High strength concrete)

summary of the steel-concrete composite tub-girder at each section designed by the AASHTO provisions.

5.3 Amount of longitudinal reinforcement and crack width

The concrete slab experiences long-term strain due to creep and dry shrinkage in the case of steel-concrete composite girders. Accordingly, an axial force will be applied to the deck slab by the long term and the short term loads. The axial force of the bottom plate considered as the reinforcement is included in the cross sectional constants when calculating the steel-concrete composite girder. However, the design basis does not provide a calculation of the crack width caused by the axial force acting on the composite girder floor plate. Therefore, it is desirable to take further consideration of the amount of reinforcement and the effect of the precast deck slab crack width. It is necessary to secure durability in joints with precast decks that tend to produce large crack width. The precast members experience some shrinkage prior to installation and aging should be considered for the period when secondary dead load occurs, so the member forces for taking into account the time effect of each loading step are calculated by CEB-FIP90. As a steel-concrete composite girder, the final shrinkage rate, ε_s applied is 27×10^{-5} and the creep coefficient ϕ_1 applied is 2.0. Fig. 15 indicates the axial force applied on the deck slab for each span length.

The longitudinal loop joints of the precast deck slab should be carefully handled because there is a high risk of cracking. The concrete strength of the deck slab was 30 MPa, the strength of the reinforcement was 400 MPa, the clearance of the joint was 350 mm, and the overlap of the rebar was 275 mm. If filler concrete is used with the same strength as the precast deck slab, the crack width equation proposed in this paper significantly increases the predicted crack width compare to the general part of the precast floor plate, as shown in Fig. 16. Therefore, the width of the crack can be controlled to a similar level as the crack width of the general part using high-strength concrete (100 MPa). By using the modified crack width equation and high-strength concrete as a filler, the crack width was reduced from 0.45 mm (uncontrolled) to 0.29 mm (controlled). Fig. 17 is a result of the crack width control at the precast connection using high strength concrete with modified crack width equation of precast joints derived from this study. It shows the crack width at the precast element, the crack width at the precast joint, and the steel ratios.

6. Discussion

The study was performed by testing the precast deck specimens. The crack width evaluation equation was derived from the results of nine specimens, each had different conditions. The test results show slight differences in the trends of each test results. This can be improved by performing additional test sampling for each condition. Additional experiments will also increase the reliability of the derived equation.

The longitudinal crack width of the longitudinal connection of the composite girder deck was not tested with a full bridge but the conditions and behavior of the precast deck test and of the actual bridge deck are not completely different. This study is deemed applicable to study the crack width calculation equation of an actual bridge even if it is not based on the entire bridge loading test. Additionally, in section 3.2 the relationship between cracking moment and

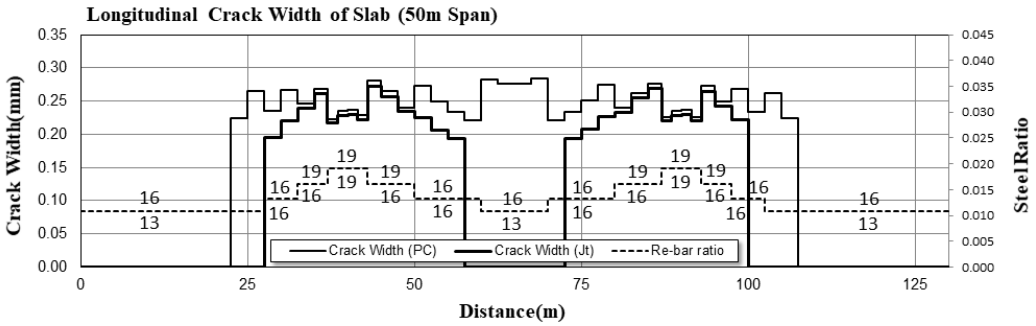

(a) 50 m span

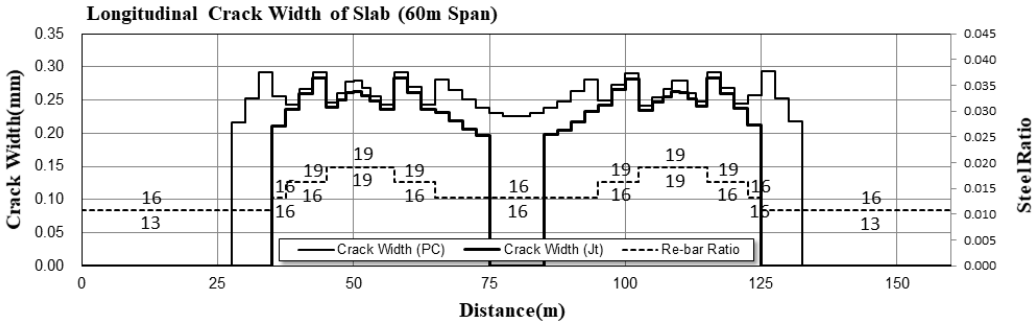

(b) 60 m span

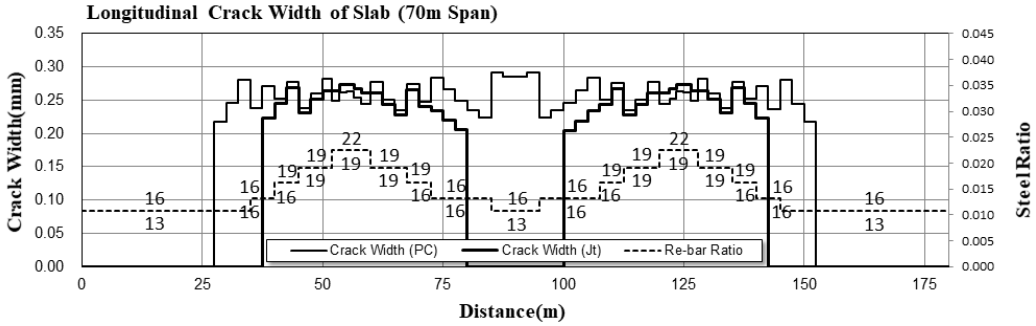

(c) 70 m span

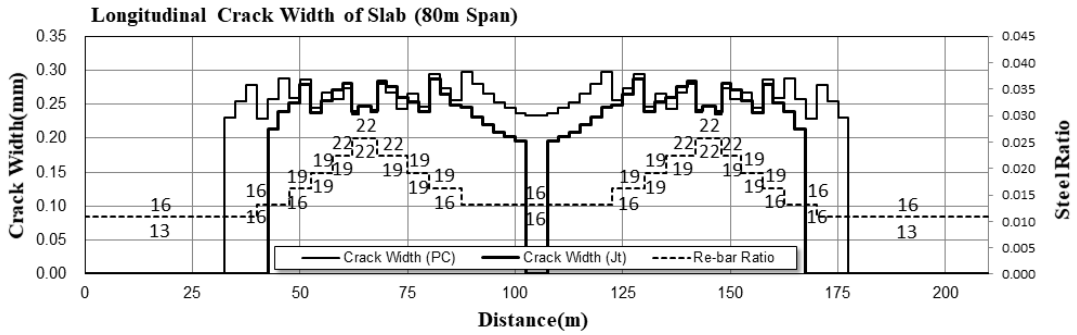

(d) 80 m span

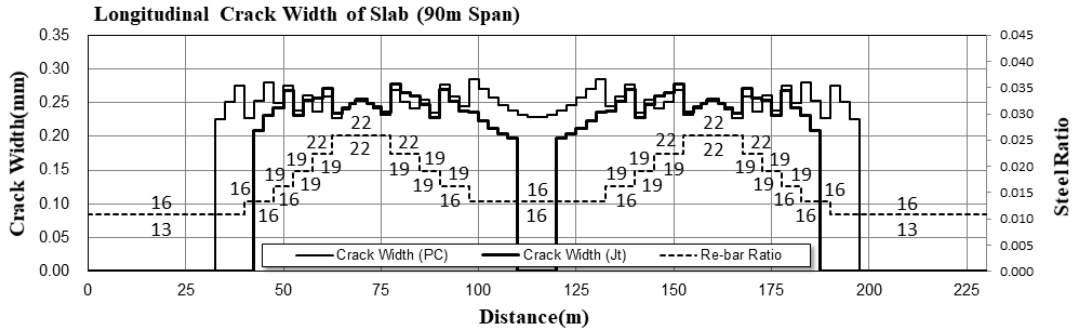

(e) 90 m span

Fig. 17 Slab crack width controlled by high strength filler according to main span length

joint distances was discussed. As the interface section is placed farther from the maximum moment section, the induced moment becomes smaller. Thus, the crack strength/resistance performance of the specimen is increased. While wider joint distances is advantageous for lower moment, workability on-site is diminished. Thus, joint distances should be minimized while satisfying the required cracking strength/resistance.

7. Conclusions

This experimental study was performed to establish the validity of the design code for calculating the crack width of precast deck loop joints with varying concrete strengths and loop joint widths. The conclusions from the experimental study are as follows:

- All experiment results showed significant ductility and reasonable extreme strength. The extreme strength of specimens filled with high-strength concrete was 78% higher than the calculated value, while for specimens filled with general strength concrete, extreme strength was 44% higher.
- The specimen having 250 mm joint width would result in excessive crack width while wider joint width exhibited increased crack resistance. The specimens with loop joints filled with high-strength concrete demonstrated better performance in terms of cracks caused by the induced loads.

A modified crack width equation developed based on observed details of loop joints can be used to account for increased crack width at the interface of precast decks.

- Because cracks are concentrated at the interface of the precast slab and filler, the maximum crack spacing equation is modified to predict larger width than at the connection spacing areas.
- Current design provisions to calculate the crack width failed to provide an adequate assessment for the precast loop joints. The modified crack width equation was able to predict the increase in the crack width at the precast joints.
- If precast decks are used in a steel-concrete composite girder, a precise evaluation is required, as cracks can be caused and durability of the bridge may be reduced by creep and shrinkage. This study was able to control crack width with a developed modified crack width equation and by using high-strength concrete filler concrete.

The use of high-performance concrete on loop joints to minimize the spacing of precast joints can be considered as an effective means to control the crack widths concentrated at the precast interface, although additional empirical studies are needed to evaluate the usefulness of the proposed modified crack width equation for loop precast joints.

Acknowledgment

This research was supported by a grant (19SCIP-B128570-03) from Smart Civil Infrastructure Research Program funded by Ministry of Land, Infrastructure and Transport of Korean Government and was also supported by the Chung-Ang University research grant in 2019.

References

AASHTO LRFD (2013), AASHTO LRFD Bridge Design Specifications, American Association of State Highway and Transportation Officials, Washington, D.C., USA.

ACI 318-14 (2014), Building Code Requirements for Structural Concrete and Commentary and Notes, American Concrete Institute, ACI Committee 318, Detroit, USA.

Bazant, Z.P. and Oh, B.H. (1983), "Spacing of cracks in reinforced concrete", *J. Struct. Eng.*, ASCE, **109**(9), 2066-2085. https://doi.org/10.1061/(ASCE)0733-9445(1983)109:9(2066).

Beeby, A.W. (1970), "An investigation of cracking in slabs spanning one way", Cement and Concrete Association, Technical Report 42.433, London, UK.

Beeby, A.W. (1971), "Prediction and control of flexural cracking in reinforced concrete members, cracking, deflection and ultimate load of concrete slab systems", American Concrete Institute, SP-20.

Beeby, A.W. (1979), "The prediction of crack widths in hardened concrete", *Struct. Eng.*, **57A**(1), 9-17.

CEB (1993), CEB-FIP Model Code 1990, Comité Euro-International Du Béton, Thomas Telford Services Ltd., London, UK.

Creazza, G. and Russo, S. (1999), "A new model for predicting crack width with different percentages of reinforcement and concrete strength classes", *Mater. Struct.*, **32**, 520-524. https://doi.org/10.1007/BF02481636.

DIN (1978), DIN 1045, Concrete and Reinforced Concrete Structures, Design and Construction (Beton und Stahlbetonban-Bemessung und Ausfuhrung), Deutsches Institut fur Normung e. V., Berlin, Germany.

EN 1992-1-1 (2005), Eurocode 2-Design of Concrete Structures-Part 1–1: General Rules and Rules for Buildings, European Committee for Standardization.

Gillen, S., Gancarz, D. and Tayabji, S.D. (2018), Precast Concrete Panels for Rapid Full-Depth Repair of CRC Pavement to Maintain Continuity of Longitudinal Reinforcement: [techbrief] (No. FHWA-HIF-18-050), Federal Highway Administration, USA.

Hallmark, R., White, H. and Collin, P. (2012), "Prefabricated bridge construction across Europe and America", *Am. Soc. Civil Eng.*, **17**(3), 82-92. https://doi.org/10.1061/(ASCE)SC.1943-5576.0000116.

Ji, SW. (2014) "Structural performance of connections in decked bulb tee girder bridges", Master Thesis, Chung-Ang University, South Korea.

Joergensen, H. and Hoang, L. (2013), "Tests and limit analysis of loop connections between precast concrete elements loaded in tension", *Eng. Struct.*, **52**, 558-569. https://doi.org/10.1016/j.engstruct.2013.03.015.

Joergensen, H.B. and Hoang, L.C. (2015), "Strength of loop connections between precast bridge decks loaded in combined tension and bending", *Struct. Eng. Int.*, **25**(1), 71-80. https://doi.org/10.2749/101686614X14043795570697.

Kim, D.H., Choi, J.W., Kim, H.Y. and Park, S.K. (2013), "An experimental study on behavior of transverse connection appropriate for modular girder bridge", *Int. J. Civil Environ. Struct. Constr. Arch. Eng.*, **7**(5), 358-366.

Kim, D.W. and Shin, J.R. (2016), "An experimental study on the flexural performance of modular slab connections with loop joints", *J. Korea Academia-Indus. Coop. Soc.*, **17**(1), 459-467. https://doi.org/10.5762/KAIS.2016.17.1.459.

Lewis, S. (2009), "Experimental investigation of precast bridge deck joints with U-bar and headed bar joint details", University of Tennessee, Knoxville, USA.

Ma, Z.J., Cao, Q., Chapman, C.E., Burdette, E.G. and French, C.E.V. (2012), "Longitudinal joint details with tight bend diameter U-bars", *ACI Struct. J.*, **109**(6), 815-824.

Ryu, H.K., Kim, Y.J. and Chang, S.P. (2007), "Crack control of a continuous composite two-girder bridge with prefabricated slabs under static and fatigue loads", *Eng. Struct.*, **29**, 851-864. https://doi.org/10.1016/j.engstruct.2006.06.021

Ryu, H.K., Kim, Y.J. and Chang, S.P. (2007), "Experimental study on static and fatigue strength of loop joints", *Eng. Struct.*, **29**(2), 145-162. https://doi.org/10.1016/j.engstruct.2006.04.014.

Shim, C.S., Chung, C.H., Kim, I.K. and Kim, Y.J. (2010), "Development and application of precast decks for composite bridges", *Struct. Eng. Int.*, **20**(2), 126-133. https://doi.org/10.2749/101686610791283623.

Shim, C.S., Kim, J.H., Chung, C.H. and Chang, S.P. (2000), "The behaviour of shear connections in composite beam with full-depth precast slab", *Proc. Inst. Civil Eng., Struct. Build.*, **140**, 101-110. https://doi.org/10.1680/stbu.2000.140.1.101.

Shim, C.S., Lee, C.D. and Ji, S.W. (2018), "Crack control of precast deck loop joint using high strength concrete", *Adv. Concrete Constr.*, **6**(5), 527-543. https://doi.org/10.12989/acc.2018.6.5.527.

Shin, D.H., Park, S.J., Oh, H.C., Kim, I.G. and Kim, Y.J. (2015), "Evaluation on flexural performance of precast bridge decks with ribbed connection", *J. Korea Inst. Struct. Mainten. Inspect.*, **19**(3), 1-9. https://doi.org/10.11112/jksmi.2015.19.3.001.

Yousif, A.A. (1995), "Field performance of full depth precast concrete panels in bridge deck reconstruction", University of Illinois at Chicago, Chicago, IL, USA.

CC